United Aircraft Research Laboratories

UNITED AIRCRAFT CORPORATION

EAST HARTFORD, CONNECTICUT

Report E910461-6

Analytical Study of Catalytic Reactors for Hydrazine Decomposition

Quarterly Progress Report No. 2
July 15 - October 14, 1966
Contract No. NAS 7-458

REPORTED BY A. S. Kesten

APPROVED BY F. S. Owen
F. S. Owen
Chief, Propulsion

DATE October 1966

NO. OF PAGES 19

COPY NO. 12

Report E910461-6

Analytical Study of Catalytic Reactors for Hydrazine Decomposition

Quarterly Progress Report No. 2

July 15 - October 14, 1966

Contract No. NAS 7-458

TABLE OF CONTENTS

Report E910461-6

Analytical Study of Catalytic Reactors for Hydrazine Decomposition

Quarterly Progress Report No. 2

July 15 - October 14, 1966

Contract No. NAS 7-458

SUMMARY

The Research Laboratories of United Aircraft Corporation under Contract NAS 7-458 with the National Aeronautics and Space Administration are performing an analytical study of catalytic reactors for hydrazine decomposition. This report summarizes work performed during the second quarter of the contract period from July 15, 1966, to October 14, 1966. Work during this reporting period has included the development and debugging of a computer program representing the steady-state microscopic model of a distributed-feed catalytic reaction chamber. The computer program provides for the simultaneous solution of the implicit integral equations describing reactant concentration and temperature profiles in the porous catalyst particles with the equations describing the variation of reactant concentrations and temperature with axial position in the interstitial phase. Several sample computer runs have been made to illustrate the use of both the program as a whole and the portion of the program which treats simultaneous heat transfer, diffusion, and chemical reaction in the porous catalyst particles.

A computer program representing the transient macroscopic model of a distributed-feed catalytic reaction chamber has also been written and is being debugged. Overall transport coefficients have been used to define the driving forces for heat and mass transfer in terms of the temperature and concentration differences between the interstitial phase and the gas phase in the interior of the catalyst particles. The ordinary and partial differential equations for the temperature and reactant concentration profiles have been formulated into a network of first order, ordinary differential equations which are solved numerically using a reasonably simple computational scheme.

INTRODUCTION

Under Contract NAS 7-458, the Research Laboratories of United Aircraft Corporation are performing analytical studies of the steady-state and transient performance characteristics of distributed-feed catalytic reactors for hydrazine decomposition. The specific objectives of this program are (a) to develop computer programs for predicting the temperature and concentration distributions in monopropellant hydrazine catalytic reactors in which hydrazine can be injected at arbitrary axial locations in the reaction chamber and (b) to perform calculations using these computer programs to demonstrate the effects of various system parameters on the performance of the reactor.

Progress previously reported in the first quarterly report (Ref. 1) included preparation of the equations comprising the steady-state macroscopic model in a form amenable to numerical solution. An iterative procedure had been developed to solve the implicit integral equations describing reactant concentration and temperature profiles in the porous catalyst particles. Numerical methods had been developed for the simultaneous solution of these equations with the equations describing the variation of reactant concentrations and temperature with axial position in the interstitial phase. In addition, work had been initiated to reduce the equations comprising the transient macroscopic model to a form amenable to numerical solution. During the present reporting period attention has been focused on extending this work to the development of computer programs representing both the steady-state microscopic model and the transient macroscopic model.

DISCUSSION

Effort during the second quarterly reporting period of Contract NAS 7-458 has involved (a) programming of the equations comprising the steady-state microscopic model, (b) debugging the steady-state program and running sample calculations to illustrate the use of both the program as a whole and the portion of the program which treats simultaneous heat transfer, diffusion, and chemical reaction in the porous catalyst particles, (c) formulating the equations comprising the transient macroscopic model into a network of first order, ordinary differential equations which can be solved numerically using a reasonably simple computational scheme, (d) programming of the equations comprising the transient model, and (e) working toward the establishment of kinetics information for use in both the steady-state and transient programs. This effort is described in detail in succeeding sections of this report.

Steady-State Microscopic Model

In the steady-state microscopic model the simultaneous processes of heat transfer, diffusion, and chemical reaction within the porous catalyst particles are considered in an implicit integral equation for the reactant concentration at any point in the particle. This equation is derived in Ref. 1 as

$$c_p(x) = (c_p)_s - \left[\frac{1}{x} - \frac{1}{a}\right] \int_0^x \xi^2 \frac{r_{het}(c_p)}{D_p} d\xi - \int_x^a \left[\frac{1}{x} - \frac{1}{a}\right] \xi^2 \frac{r_{het}(c_p)}{D_p} d\xi \quad (1)$$

The rate of chemical reaction on the catalyst surfaces, $r_{het}(c_p)$, is given, in general, by

$$r_{het}(c_p) = k_o (c_p)_s^{1-n} (c_p)^n \exp\left\{\gamma\beta \left(1 - c_p/(c_p)_s\right) \Big/ \left[1 + \beta\left(1 - c_p/(c_p)_s\right)\right]\right\} \quad (2)$$

where the parameters, k_o, n, γ, and β are defined in the list of symbols. Equations (1) and (2) are solved in an iterative fashion in a subroutine contained in the main program representing the steady-state microscopic model. Sample calculations have been made to illustrate the use of this subroutine for computing concentration profiles in the porous catalyst particles, the associated temperature profiles, and the concentration gradients at the particle surface. The subroutine was run for values of the reaction rate constant, k_o, between 2.0 sec^{-1} and 2.0 x 10^6 sec^{-1}, and for $\beta = 0.171$, $\gamma = 18.3$, $D_p = 0.84 \times 10^{-5}$ ft/sec^2, $a = 0.005$ ft, $n = 1$, and $(c_p)_s = 0.357$ lb/ft^3. The values chosen for β, γ, D_p, n, and $(c_p)_s$ are reasonable for the decomposition of hydrazine within Shell 405 catalyst pellets. The resulting concentration profiles are plotted for each reaction rate constant in Fig. 1 and the associated

temperature profiles are shown in Fig. 2. The concentration gradient at the particle surface is plotted as a function of the reaction rate constant in Fig. 3.

If the reactant concentration at the surface of the particle, $(c_p)_s$, is equal to the concentration in the interstitial phase, c_i, Eqs. (1) and (2) can be solved simultaneously with the equations shown in Ref. 1 describing the changes in enthalpy and reactant concentrations in the interstitial phase with axial distance to yield the steady-state temperature and concentration profiles in the reaction chamber. In the liquid region of the chamber, for example, it is assumed that liquid hydrazine wets the outside surface of the catalyst particles so that $(c_p)_s^{N_2H_4} = c_i^{N_2H_4}$ where $c_i^{N_2H_4}$ is the vapor concentration in equilibrium with liquid hydrazine at temperature T_i. In the vapor region of the reactor it can be shown that $(c_p)_s^{NH_3} \sim c_i^{NH_3}$ at the temperatures existing in the chamber since the rate of transport of material from the bulk fluid to the outside surface of the catalyst particles is much greater than the rate of dissociation of ammonia within the particles. However, in the case of hydrazine decomposition in the vapor region the rate of catalytic decomposition is so high that $(c_p)_s^{N_2H_4} \ll c_i^{N_2H_4}$ and the reaction rate is governed by the rate of mass transfer from the bulk vapor to the outside surface of the catalyst particles. This rate is given approximately by $(k_c c_i)^{N_2H_4}$ where the mass transfer coefficient, k_c, may be estimated from (Ref. 2)

$$k_c = \frac{0.61\,G}{\rho_i}\left(\frac{\mu}{\rho_i D_i}\right)^{-0.667}\left(\frac{G}{A_p \mu}\right)^{-0.41} \qquad (3)$$

For hydrazine decomposition in the vapor region, then, the terms $\left[D_p(dc_p/dx)_s\right]^{N_2H_4}$ in the equations in Ref. 1 describing the changes in enthalpy and reactant concentrations in the interstitial phase with axial distance are replaced by $(k_c c_i)^{N_2H_4}$.

In the liquid-vapor region the situation is somewhat more complicated since it is difficult to predict whether liquid or a combination of liquid and vapor wets the outside surface of the catalyst particles. Both of these options are presently in the computer program representing the steady-state model. In the case in which both liquid and vapor are taken to wet the particle surface, it is assumed that, at a given axial location, the fraction of the surface covered by vapor is equal to the weight-fraction of vapor present. Decomposition rates, computed assuming pure liquid surface coverage and then pure vapor coverage, are weighted accordingly.

Sample calculations have been made to illustrate the use of the computer program representing the steady-state model for computing the variation of reactant concentrations and temperatures with axial distance in the interstitial phase. The calculations apply to a reaction chamber 3 in. long with the first 0.2 in. packed with 25 to 30 mesh granular catalyst pellets ($A_p = 2100$ ft^2/ft^3) and the remainder packed with 1/8 in. x 1/8 in. cylindrical pellets ($A_p = 330$ ft^2/ft^3). The interparticle void fraction was taken as constant at 0.3. The mass flow rate, G, was

taken as constant at 3.0 lb/ft^2-sec (i.e., F = 0), the pressure, P, was taken as 100 psia, and the feed temperature was taken as 530 deg R. The kinetics assumed in the calculation were

$$r_{hom}^{N_2H_4} = 2.14 \times 10^{10}\ C_i^{N_2H_4}\ e^{-33{,}000/T_i} \qquad LB/FT^3 - SEC$$

$$r_{het}^{N_2H_4} = 10^{10}\ C_P^{N_2H_4}\ e^{-5000/T_P} \qquad LB/FT^3 - SEC$$

$$r_{het}^{NH_3} = 10^{14}\ C_P^{NH_3}\ e^{-50{,}000/T_P} \qquad LB/FT^3 - SEC$$

where T_i and T_P are in deg R. These reaction rates are reasonable for the system being considered. The resulting axial temperature profiles are plotted in Fig. 4 for both options in the liquid-vapor region. It is apparent that, using the assumed kinetics information for heterogeneous decomposition of hydrazine, the liquid-vapor region is so narrow that the choice of either of these options has negligible effect on the resulting temperature distributions. Axial concentration profiles for hydrazine, ammonia, nitrogen, and hydrogen are plotted in Fig. 5 and the fractional ammonia dissociation is plotted as a function of axial distance in Fig. 6.

Transient Macroscopic Model

In developing the transient macroscopic model, the concentrations of reactants in the interstitial phase are assumed to vary only with time and axial distance along the bed. In this system the rates of heat and mass transfer between the interstitial phase and the gas phase within the porous particles are expressed in terms of overall transfer coefficients. The reactant concentrations, C_P, and the temperature, T_P, are taken as uniform within the interior of the porous particles. In addition, it is assumed that liquid velocities are sufficiently low relative to other rate processes so that, for all practical purposes, steady-state in the liquid and liquid-vapor regions is achieved as soon as the liquid reaches a given axial location in the reactor.

The transient model is concerned then with the vapor region only, where velocities are about three orders of magnitude greater than in the liquid region. Here it is reasonable to assume that gas velocities are so great that the time lag from the entrance to the vapor region to any position z for the fluid is negligible compared with other transient effects. With this assumption the rates of change of temperature and reactant concentrations with axial distance in the interstitial phase are given by

$$\frac{\partial T_i}{\partial z} = -\frac{H^{N_2H_4}}{G\bar{C}_F} r_{hom}\delta - \frac{A_P}{G\bar{C}_F}\left[h_s\ (T_i - T_P)\right] - \frac{F}{G\bar{C}_F}\left[(h_i^v - h_F) + \bar{C}_F\ (T_i - T_{vap})\right] \qquad (4)$$

$$\frac{\partial c_i^{N_2H_4}}{\partial z} = -c_i^{N_2H_4}\left(\frac{1}{T_i}\frac{\partial T_i}{\partial z} + \frac{F}{G}\right)$$

$$+ \frac{P\bar{M}}{RGT_i}\left[F - r_{hom}\delta - A_p k_s^{N_2H_4}\left(c_i^{N_2H_4} - c_p^{N_2H_4}\right)\right] \quad (5)$$

$$\frac{\partial c_i^{NH_3}}{\partial z} = -c_i^{NH_3}\left(\frac{1}{T_i}\frac{\partial T_i}{\partial z} + \frac{F}{G}\right)$$

$$+ \frac{P\bar{M}}{RGT_i}\left[r_{hom}\delta\frac{M^{NH_3}}{M^{N_2H_4}} - A_p k_s^{NH_3}\left(c_i^{NH_3} - c_p^{NH_3}\right)\right] \quad (6)$$

$$\frac{\partial c_i^{N_2}}{\partial z} = -c_i^{N_2}\left(\frac{1}{T_i}\frac{\partial T_i}{\partial z} + \frac{F}{G}\right)$$

$$+ \frac{P\bar{M}}{RGT_i}\left[r_{hom}\delta\frac{M^{N_2}}{2M^{N_2H_4}} - A_p k_s^{N_2}\left(c_i^{N_2} - c_p^{N_2}\right)\right] \quad (7)$$

$$\frac{\partial c_i^{H_2}}{\partial z} = -c_i^{H_2}\left(\frac{1}{T_i}\frac{\partial T_i}{\partial z} + \frac{F}{G}\right)$$

$$+ \frac{P\bar{M}}{RGT_i}\left[r_{hom}\delta\frac{M^{H_2}}{2M^{N_2H_4}} - A_p k_s^{H_2}\left(c_i^{H_2} - c_p^{H_2}\right)\right] \quad (8)$$

The equations for the steady-state model analogous to Eqs. (4) through (8) are shown in Ref. 1 as Eqs. (4) through (8). The transient and steady-state equations may be compared in consistent units by dividing the gas constant, R, in Eqs. (4) through (8) of Ref. 1 by the average molecular weight, $\bar{M}$. At a given axial location the rates of change of temperature and reactant concentrations in the catalyst particles with time are given by

$$\frac{dT_p}{dt} = -\frac{1}{\rho_s C_s}\left[(H r_{het})^{N_2H_4} + (H r_{het})^{NH_3}\right] + \frac{3k_s}{a\rho_s C_s}(T_i - T_p) \quad (9)$$

$$\frac{dc_P^{N_2H_4}}{dt} = -\frac{1}{\alpha_P} r_{het}^{N_2H_4} + \frac{3k_S^{N_2H_4}}{\alpha_P a}\left(c_i^{N_2H_4} - c_P^{N_2H_4}\right) \tag{10}$$

$$\frac{dc_P^{NH_3}}{dt} = \frac{1}{\alpha_P}\left[r_{het}^{N_2H_4}\frac{M^{NH_3}}{M^{N_2H_4}} - r_{het}^{NH_3}\right] + \frac{3k_S^{NH_3}}{\alpha_P a}\left(c_i^{NH_3} - c_P^{NH_3}\right) \tag{11}$$

$$\frac{dc_P^{N_2}}{dt} = \frac{1}{\alpha_P}\left[r_{het}^{N_2H_4}\frac{M^{N_2}}{2M^{N_2H_4}} + r_{het}^{NH_3}\frac{M^{N_2}}{2M^{NH_3}}\right] + \frac{3k_S^{N_2}}{\alpha_P a}\left(c_i^{N_2} - c_P^{N_2}\right) \tag{12}$$

$$\frac{dc_P^{H_2}}{dt} = \frac{1}{\alpha_P}\left[r_{het}^{N_2H_4}\frac{M^{H_2}}{2M^{N_2H_4}} + r_{het}^{NH_3}\frac{3M^{H_2}}{2M^{NH_3}}\right] + \frac{3k_S^{H_2}}{\alpha_P a}\left(c_i^{H_2} - c_P^{H_2}\right) \tag{13}$$

Equations (4) through (13) must be solved simultaneously for the variation of temperatures and reactant concentrations with time and axial position in the reactor. Partial differential Eqs. (4) through (8) can be treated as ordinary differential equations by integrating them at constant time. This can be accomplished, together with integrating Eqs. (9) through (13) at fixed axial positions, by establishing a network containing fixed time intervals and intervals of axial distance. Reactant concentrations and temperatures in the interstitial phase and in the catalyst particles are then computed at the i th time and j th axial distance from

$$(T_P)_{i,j} = (T_P)_{i-1,j} + \left(\frac{dT_P}{dt}\right)_{i-1,j}\Delta t \tag{14}$$

$$(c_P)_{i,j}^{N_2H_4} = (c_P)_{i-1,j}^{N_2H_4} + \left(\frac{dc_P}{dt}\right)_{i-1,j}^{N_2H_4}\Delta t \tag{15}$$

$$(c_P)_{i,j}^{NH_3} = (c_P)_{i-1,j}^{NH_3} + \left(\frac{dc_P}{dt}\right)_{i-1,j}^{NH_3}\Delta t \tag{16}$$

$$(C_P)_{i,j}^{N_2} = (C_P)_{i-1,j}^{N_2} + \left(\frac{dC_P}{dt}\right)_{i-1,j}^{N_2} \Delta t \tag{17}$$

$$(C_P)_{i,j}^{H_2} = (C_P)_{i-1,j}^{H_2} + \left(\frac{dC_P}{dt}\right)_{i-1,j}^{H_2} \Delta t \tag{18}$$

$$(T_i)_{i,j} = (T_i)_{i,j-1} + \left(\frac{\partial T_i}{\partial z}\right)_{i,j-1} \Delta z \tag{19}$$

$$(C_i)_{i,j}^{N_2H_4} = (C_i)_{i,j-1}^{N_2H_4} + \left(\frac{\partial C_i}{\partial z}\right)_{i,j-1}^{N_2H_4} \Delta z \tag{20}$$

$$(C_i)_{i,j}^{N_2} = (C_i)_{i,j-1}^{N_2} + \left(\frac{\partial C_i}{\partial z}\right)_{i,j-1}^{N_2} \Delta z \tag{21}$$

$$(C_i)_{i,j}^{NH_3} = (C_i)_{i,j-1}^{NH_3} + \left(\frac{\partial C_i}{\partial z}\right)_{i,j-1}^{NH_3} \Delta z \tag{22}$$

$$(C_i)_{i,j}^{H_2} = (C_i)_{i,j-1}^{H_2} + \left(\frac{\partial C_i}{\partial z}\right)_{i,j-1}^{H_2} \Delta z \tag{23}$$

Simultaneous solution of Eqs. (14) through (23) together with Eqs. (4) through (13) will yield the temperature and concentration profiles in the reaction chamber as functions of time. A computer program representing these equations has been written and is presently being debugged.

Kinetics Information

Work is in progress on the establishment of kinetics information for use in both the steady-state and transient programs. A literature survey has provided sufficient information for estimating the rate laws governing homogeneous, vapor-phase decomposition of hydrazine (Refs. 3, 4, and 5) and heterogeneous, vapor-phase decomposition of ammonia (Refs. 6 and 7) on materials resembling the Shell 405 catalyst (e.g., platinum). Similar information relating to the catalytic decomposition of hydrazine is not available. However, a company-funded program is in progress which may provide limited data on the rates of heterogeneous, vapor-phase decomposition of hydrazine on platinum-family metals. Small-scale laboratory experiments are being performed with the objective of providing estimates of the activation energy and the order of the catalytic decomposition reaction.

REFERENCES

1. Kesten, A. S.: Analytical Study of Catalytic Reactors for Hydrazine Decomposition. United Aircraft Research Laboratories Report E910461-3, Contract NAS 7-458, July 1966.

2. Bird, R. B., W. E. Stewart, and E. N. Lightfoot: Transport Phenomena. John Wiley & Sons, Inc., New York, 1960.

3. Eberstein, I. J., and I. Glassman: The Gas-Phase Decomposition of Hydrazine a and Its Methyl Derivations. Tenth Symposium (International) on Combustion, The Combustion Institute, Pittsburgh, 1965, pp. 365-374.

4. McHale, E. T., B. E. Knox, and H. B. Palmer: Determination of the Decomposition Kinetics of Hydrazine Using a Single-Pulse Shock Tube. Tenth Symposium (International) on Combustion, The Combustion Institute, Pittsburgh, 1965, pp. 341-351.

5. Michel, K. W., and H. GG. Wagner: The Pyrolysis and Oxidation of Hydrazine Behind Shock Waves. Tenth Symposium (International) on Combustion, The Combustion Institute, Pittsburgh, 1965, pp. 353-364.

6. Logan, S. R., and C. Kemball: The Catalytic Decomposition of Ammonia on Evaporated Metal Films. Transactions of the Faraday Society, 56, 1960, pp. 144-153.

7. Melton, C. E., and P. H. Emmett: Transient Species Observed in the Catalyzed Decomposition of Ammonia. J. of Physical Chemistry, 68, 1964, pp. 3318-3324.

LIST OF SYMBOLS

a	Radius of spherical particle
A_P	Total external surface of catalyst particle per unit volume of bed
c_i	Reactant concentration in interstitial fluid
c_P	Reactant concentration in gas phase within the porous particle
C_f	Specific heat of fluid in the interstitial phase
$\overline{C}_f$	Average specific heat of fluid in the interstitial phase
C_s	Specific heat of catalyst particle
D_i	Diffusion coefficient of reactant gas in the interstitial fluid
D_P	Diffusion coefficient of reactant gas in the porous particle
F	Rate of feed of reactant into the system
G	Mass flow rate
h	Enthalpy
h_s	Overall heat transfer coefficient
H	Heat of reaction (negative for exothermic reaction)
k_c	Mass transfer coefficient (used in steady-state model)
k_o	Reaction rate constant, equals $\alpha e^{-\gamma}$
k_s	Overall mass transfer coefficient (used in transient model)
K_P	Thermal conductivity of the porous catalyst particle
M	Molecular weight
$\overline{M}$	Average molecular weight
n	Order of decomposition reaction

P	Chamber pressure
Q	Activation energy
r_{het}	Rate of (heterogeneous) chemical reaction on the catalyst surfaces
r_{hom}	Rate of (homogeneous) chemical reaction in the interstitial phase
R	Gas constant
t	Time
T	Temperature
x	Radial distance from the center of the spherical catalyst particle
z	Axial distance
α	Preexponential factor in rate equation
α_P	Intraparticle void fraction
β	Equals $\frac{-(C_P)_S \, H \, D_P}{K_P (T_P)_S}$
γ	Equals $Q / R(T_P)_S$
δ	Interparticle void fraction
μ	Viscosity of interstitial fluid
ρ_i	Density of interstitial fluid
ρ_S	Bulk density of catalyst particle

Subscripts

F	Refers to feed
i	Refers to interstitial phase
P	Refers to gas within the porous catalyst particle
S	Refers to surface of catalyst particle

Superscripts

L	Refers to liquid at vaporization temperature
V	Refers to vapor at vaporization temperature

FIG. 1

EFFECT OF REACTION RATE CONSTANT ON CONCENTRATION PROFILE WITHIN CATALYST PARTICLE

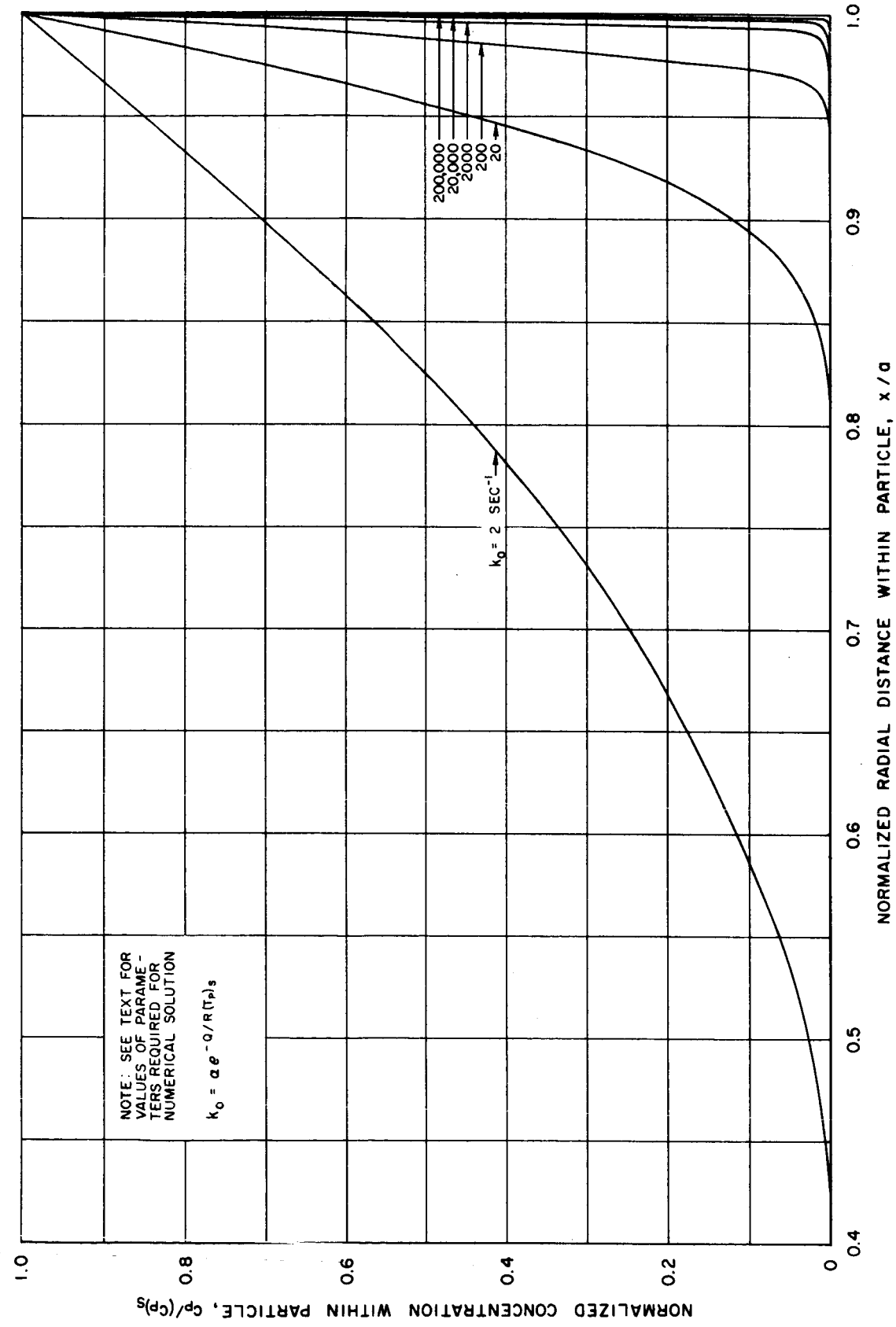

FIG. 2

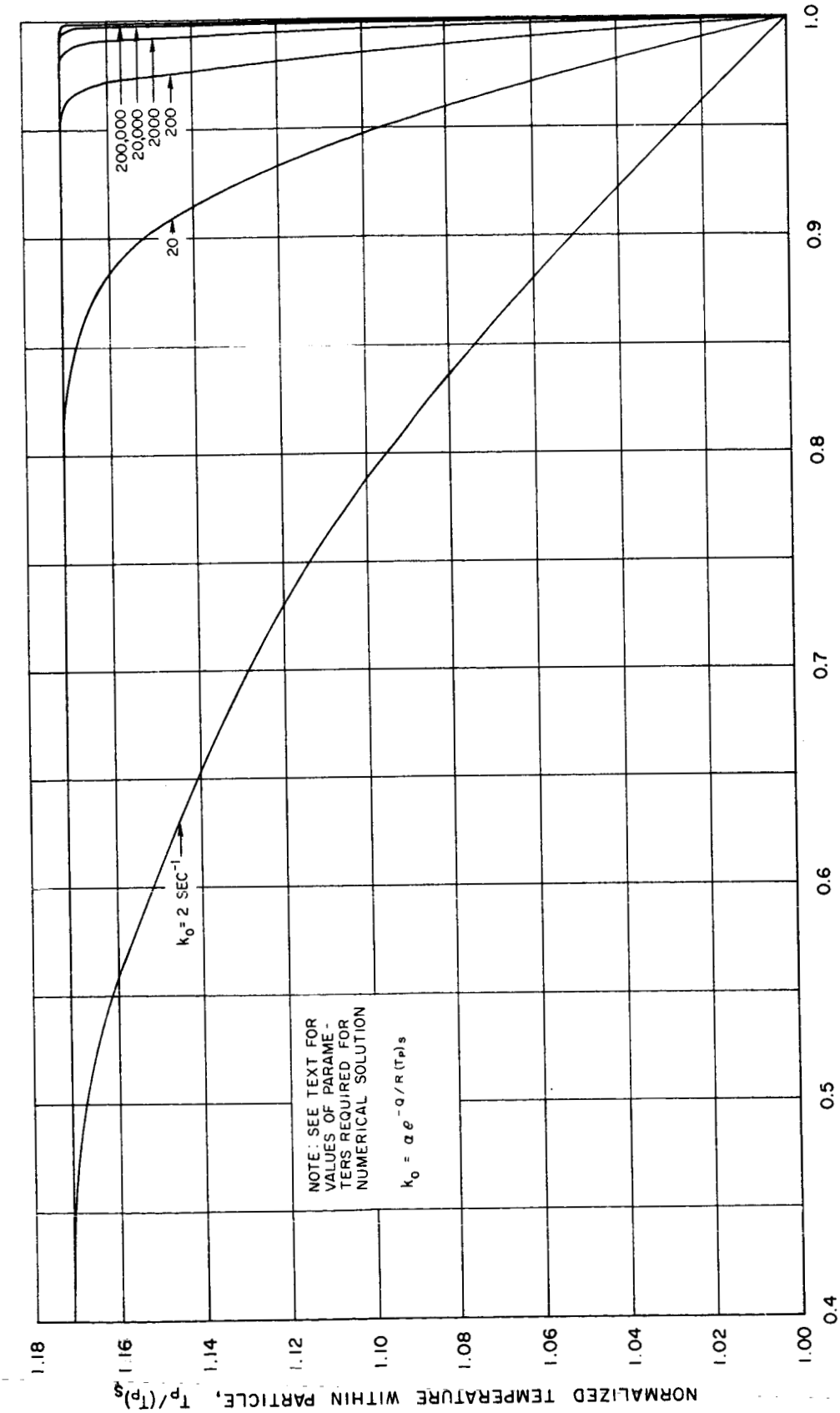
EFFECT OF REACTION RATE CONSTANT
ON TEMPERATURE PROFILE WITHIN CATALYST PARTICLE
NORMALIZED TEMPERATURE WITHIN PARTICLE, $T_p/(T_p)_s$
NORMALIZED RADIAL DISTANCE WITHIN PARTICLE, x/a
1.18
1.16
1.14
1.12
1.10
1.08
1.06
1.04
1.02
1.00
0.4
0.5
0.6
0.7
0.8
0.9
1.0
200,000
20,000
2000
200
20
k_0 = 2 SEC^{-1}
NOTE: SEE TEXT FOR VALUES OF PARAMETERS REQUIRED FOR NUMERICAL SOLUTION
$k_0 = \alpha e^{-Q/R(T_p)_s}$

FIG. 3

VARIATION OF CONCENTRATION GRADIENT AT PARTICLE SURFACE WITH REACTION RATE CONSTANT

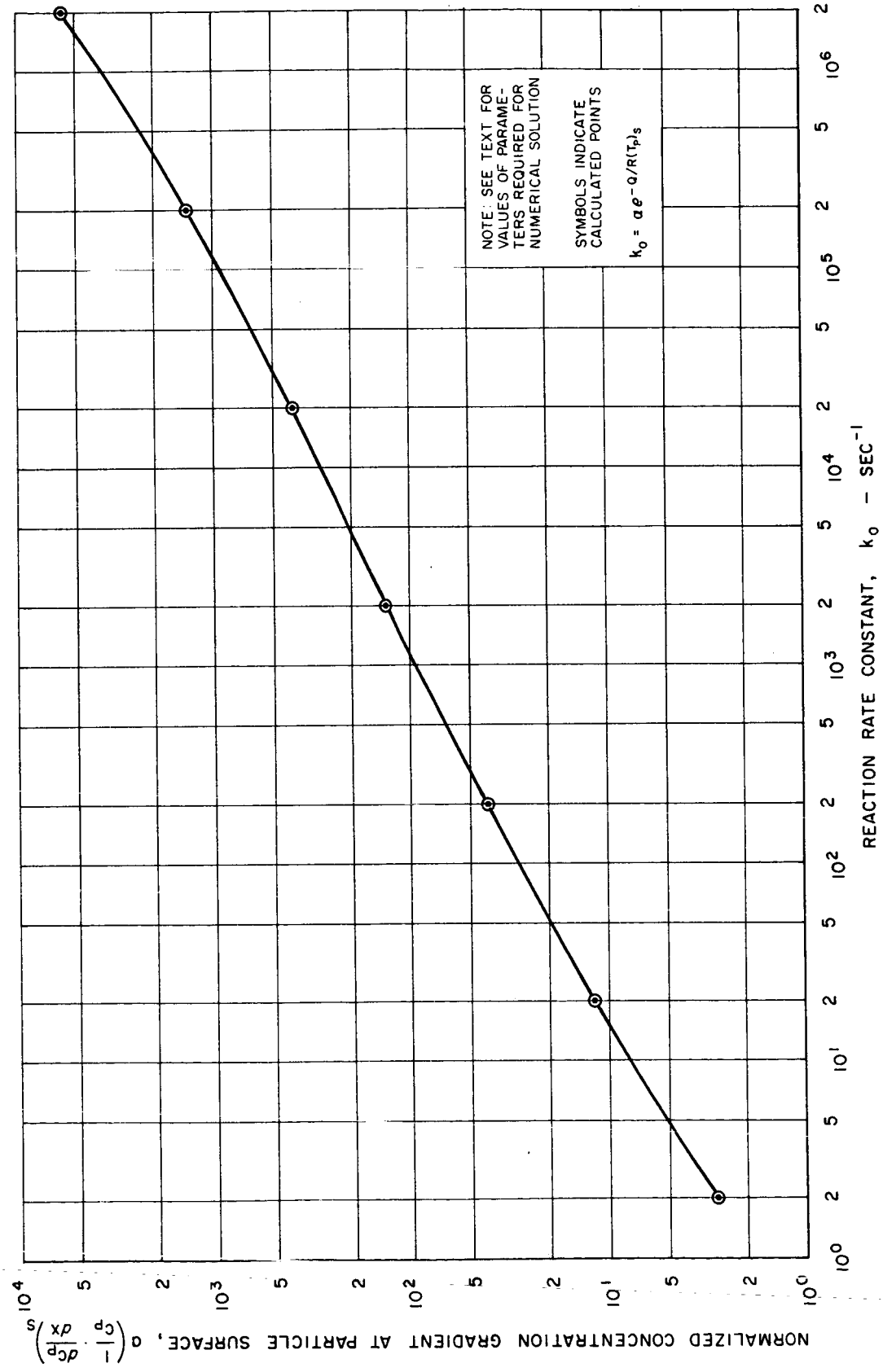

FIG. 4

STEADY-STATE AXIAL PROFILE OF TEMPERATURE IN INTERSTITIAL PHASE

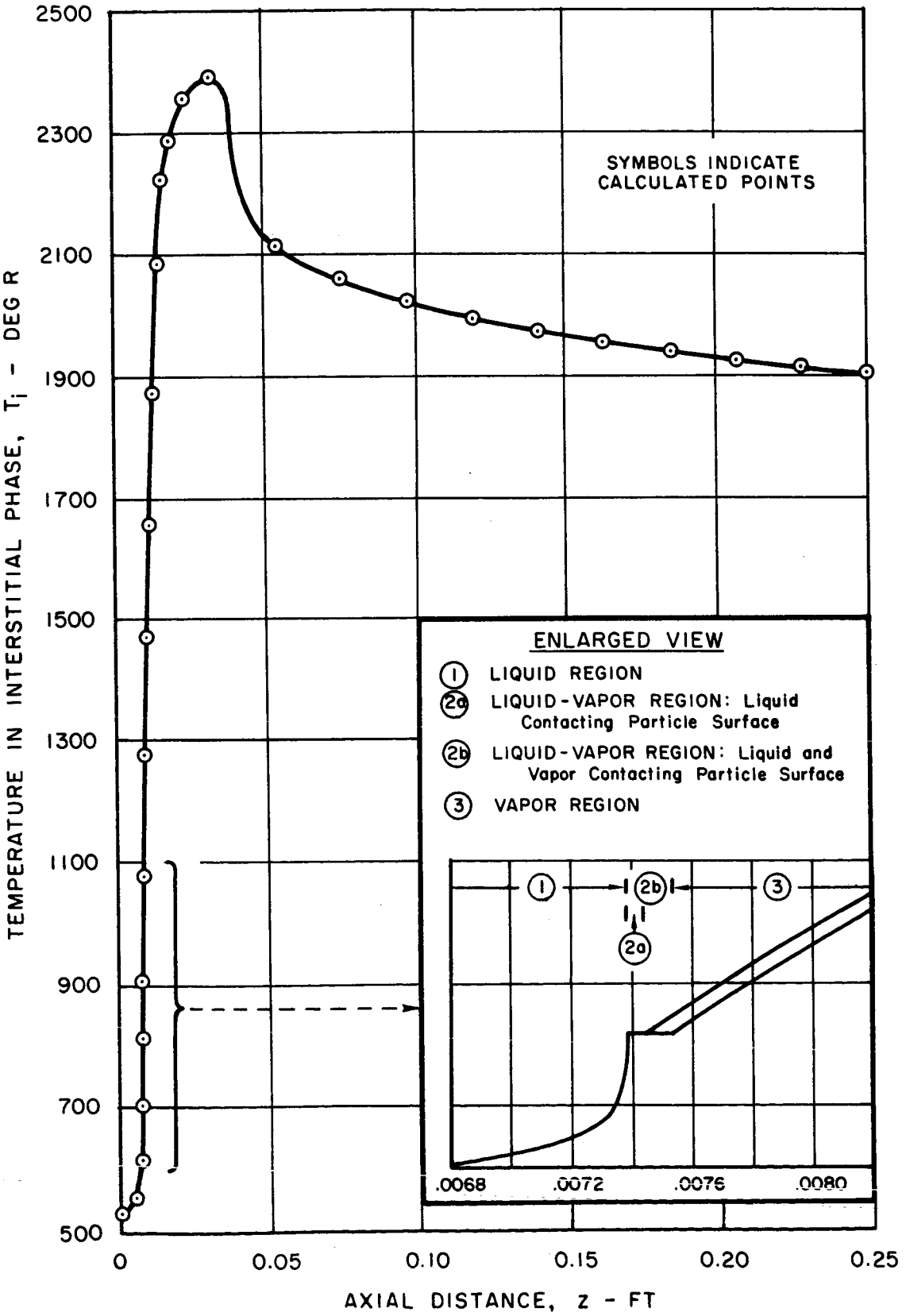

FIG. 5

STEADY-STATE AXIAL PROFILE OF MOLE-FRACTIONS OF REACTANTS IN INTERSTITIAL PHASE

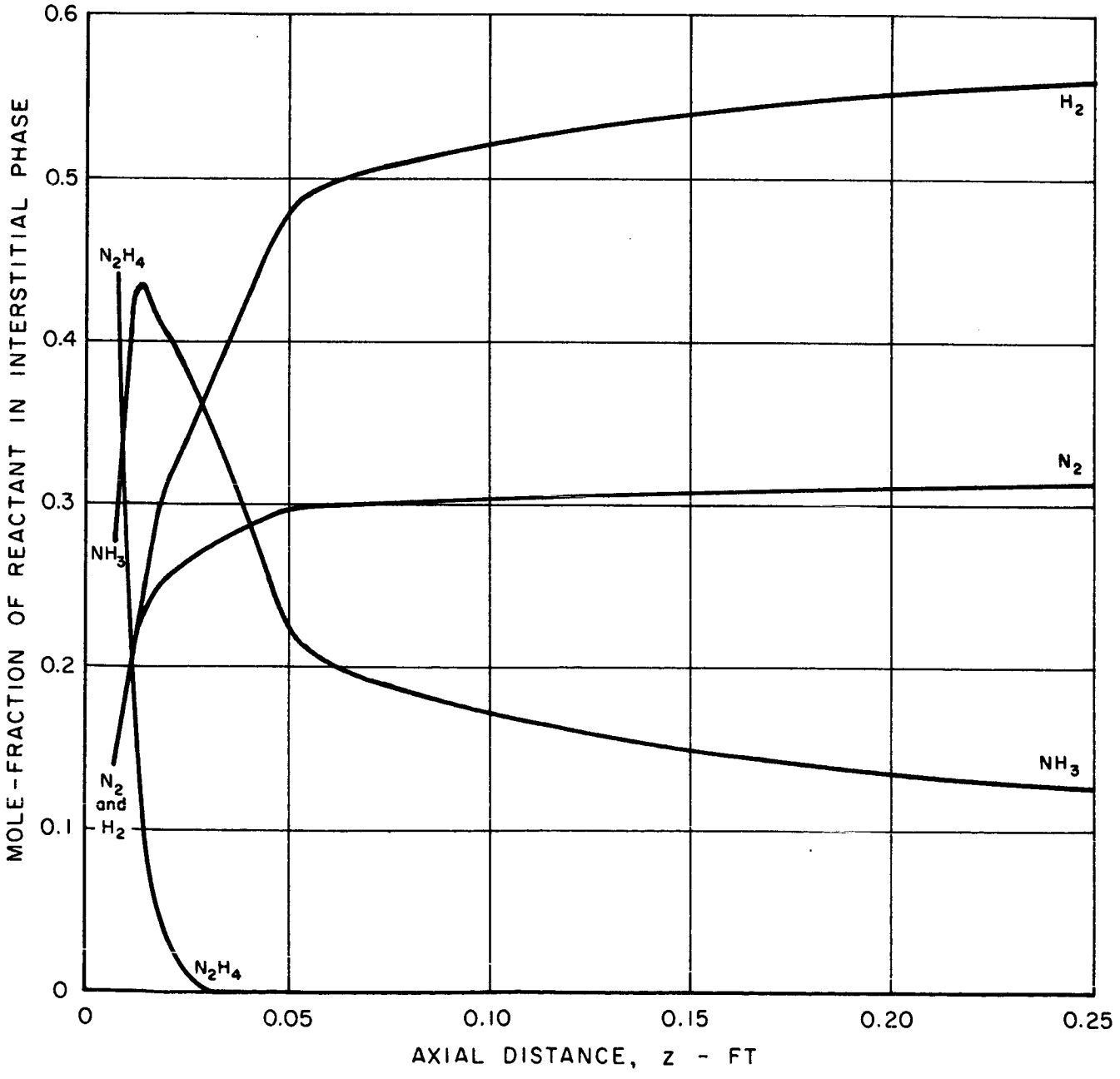

FIG. 6

STEADY-STATE AXIAL PROFILE OF FRACTIONAL AMMONIA DISSOCIATION

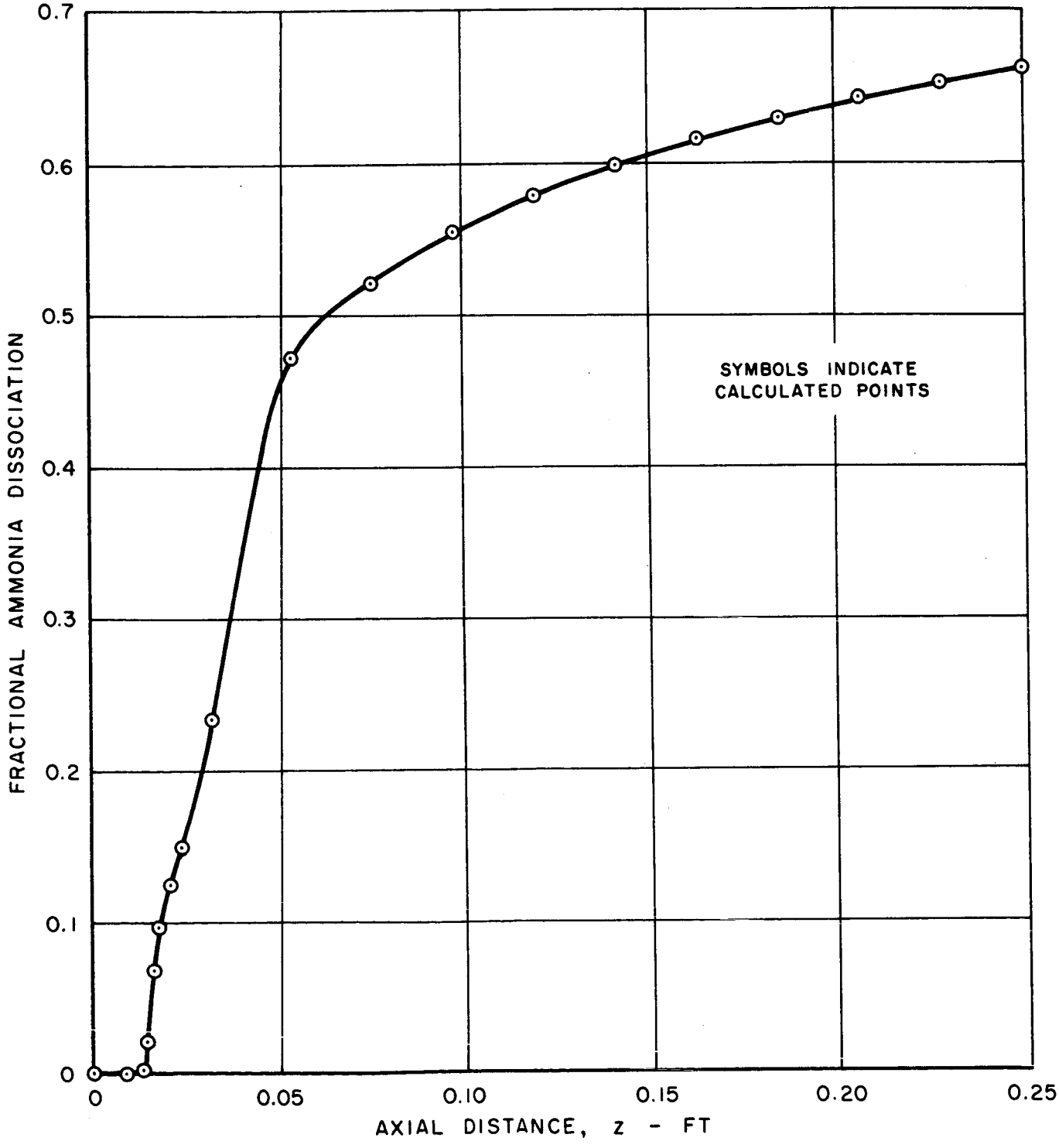

ESTIMATED PROGRESS SCHEDULE

CUMULATIVE TOTAL EXPENDITURES *

NAS 7 - 458

*EXCLUSIVE OF FEE

TOTAL EXPENDITURES (DOLLARS): 56,738

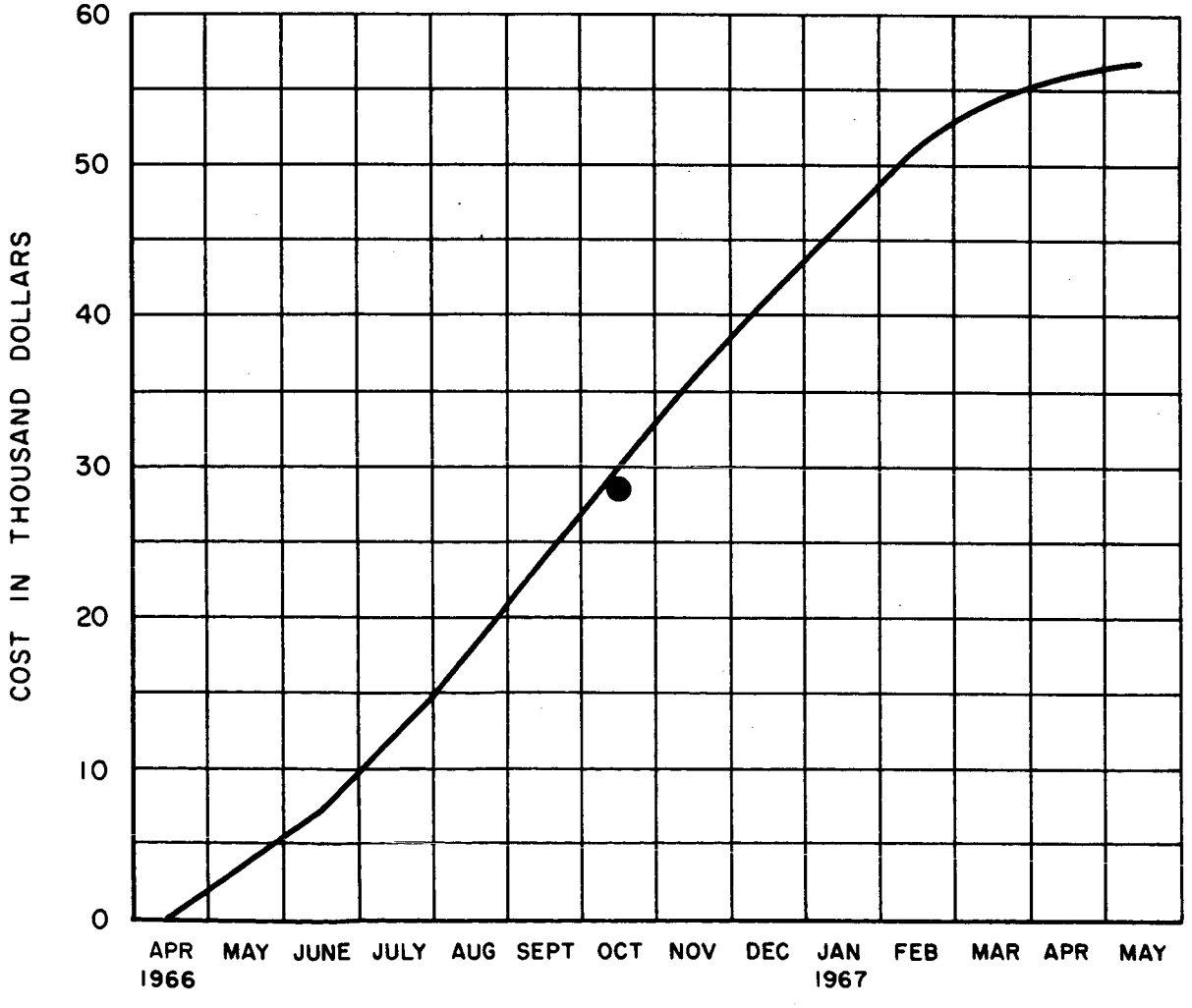

ENCLOSURE B

ESTIMATED PROGRESS SCHEDULE

CUMULATIVE DIRECT LABOR

NAS 7 - 458

TOTAL MAN-HOURS: 4790

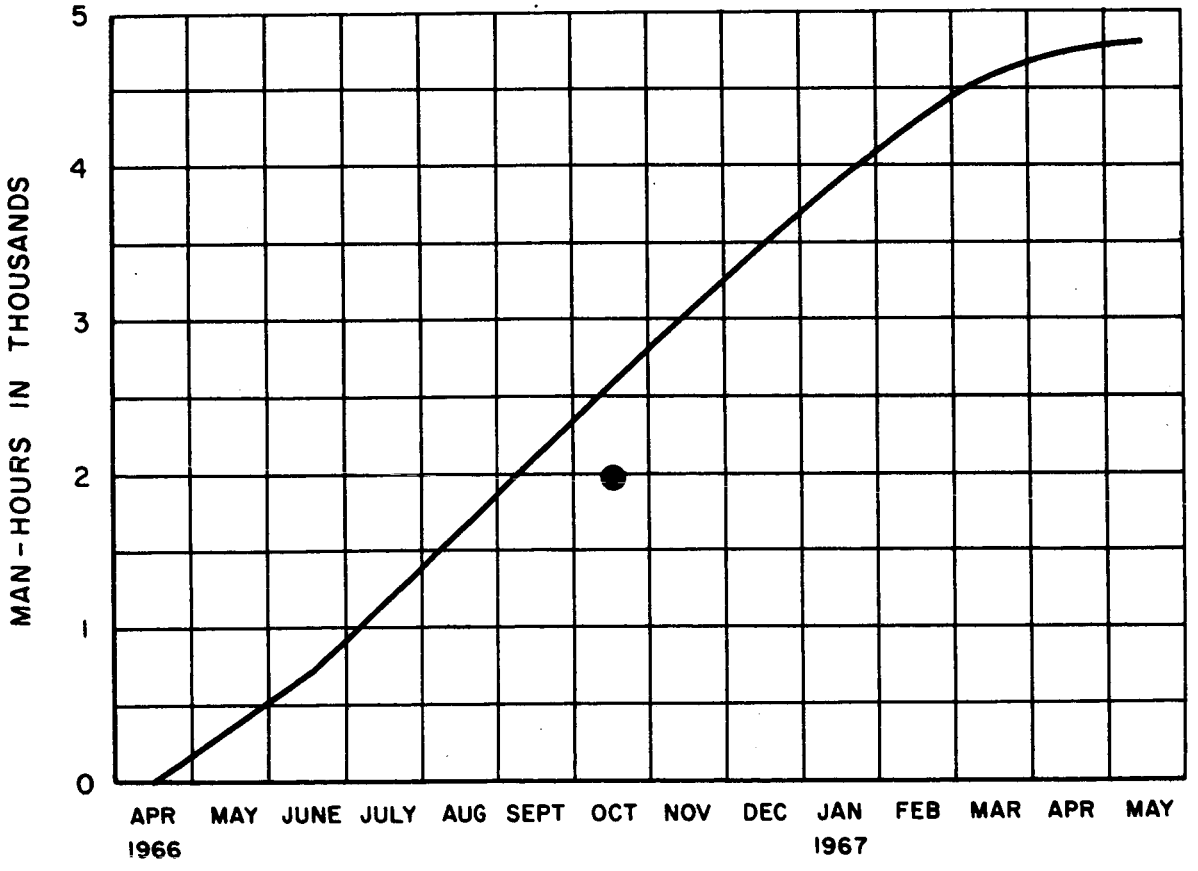

DISTRIBUTION LIST FOR MONTHLY/QUARTERLY REPORTS
(Contract NAS 7-458)

Addressee	No. of Copies
National Aeronautics and Space Administration NASA Resident Office Jet Propulsion Laboratory 4800 Oak Grove Drive Pasadena, California 91103A Attn: Mr. James S. Evans Contracting Officer, T-93	3
Jet Propulsion Laboratory 4800 Oak Grove Drive Pasadena, California 91103 Attn: Mr. T. W. Price	1
AFRPL (RPRED) Edwards Air Force Base, California 93523 Attn: Mr. K. O. Rimer	1
U. S. Naval Ordnance Test Station China Lake, California 93557 Attn: Mr. J. O. Dake, Code 4505	1
NASA Headquarters Washington, D. C. 20546 Attn: Mr. R. H. Rollins, II, Code RPX	1
NASA Headquarters Washington, D. C. 20546 Attn: Dr. R. Levine, Code RPL	1
NASA Headquarters Washington, D. C. 20546 Attn: Mr. C. H. King, Code MAT	1
National Aeronautics and Space Administration Manned Spacecraft Center Houston, Texas 77058 Attn: Mr. H. A. Pohl	1
National Aeronautics and Space Administration Lewis Research Center 21000 Brookpark Road Cleveland, Ohio 44135 Attn: Mr. I. A. Johnsen	1

DISTRIBUTION LIST FOR MONTHLY/QUARTERLY REPORTS
(Contract NAS 7-458)

Addressee	No. of Copies
National Aeronautics and Space Administration Langley Research Center Langley Station Hampton, Virginia 23365 Attn: Mr. Robert L. Swain	1
Jet Propulsion Laboratory 4800 Oak Grove Drive Pasadena, California 91103 Attn: Mr. D. D. Evans	1
National Aeronautics and Space Administration Goddard Space Flight Center Greenbelt, Maryland 20771 Attn: Mr. D. J. Grant	1
National Aeronautics and Space Administration George C. Marshall Space Flight Center Redstone Arsenal Huntsville, Alabama 35812 Attn: Mr. J. Thompson	1
Air Force Office of Scientific Research Washington, D. C. 20546 Attn: Lt. Col. John Donovan	1
Scientific and Technical Information Facility P. O. Box 5700 Bethesda, Maryland 20014 Attn: NASA Representative, Code CRT	1